بیست و سومین کنفرانس اپتیک و فوتونیک و نهمین کنفرانس مهندسی و فناوری فوتونیک ایران
دانشگاه تربیت مدرس
۱۲-۱۴ بهمن ۱۳۹۵
23rd Iranian Conference on Optics and Photonics and 9th Conference on Photonics Engineering and Technology
Tarbiat Modares University, Tehran, Iran
January 31- February 2, 2017

Refractive Index Correction in Optical Coherence Tomography Images

Zahra Turani[1], Emad Fatemizadeh[1], Mohammadreza Nasiriavanaki[2]
[1] Department of Electrical Engineering, Sharif University of Technology, Tehran, Iran
[2] Department of Dematology, College of Engineering and school of Medicine Wayne State University
[2] Karmanos Cancer institute, College of Engineering and school of Medicine Wayne State University

Abstract- Optical coherence tomography (OCT) imaging is a high resolution and non-invasive imaging modality that provides cross-sectional images of a tissue. The time of fly in the signal processing of the OCT system is calculated based on a constant refractive index. Different layers of the complex tissues however have different refractive indices. This issue prompts pixels in the image to be misplaced and that makes it difficult for the physicians to have an accurate diagnosis of abnormalities based on OCT imaging. In this paper, we propose a novel post-processing method to correct for the refractive index. The proposed method is based on imaging a tissue to which a needle has penetrated.
Keywords: Optical coherence tomography, dermatology, image enhancement, refractive index correction, optical imaging.

1 Introduction

Light beams in complex tissues are affected by optical properties of the tissue. The beams will then experience refraction, scattering and absorption[2, 3]. A difference in refractive indices of various tissues makes the light beam to be refracted at the boundary of the two layers. Thus, in the OCT images, the beam is deflected as soon as it enters the tissue; the deflection differs in different layers of the tissue. Therefore, it is important to know the refractive indices of the layers and use it in the image construction phase of OCT imaging. In practice it is not possible to find the exact value of refractive indices of the tissue layers and thus, an approximated constant refractive index is considered for the entire tissue. As a result, the location of pixels are misplaced. Various methods have been developed to find the refractive index of tissue layers, known as refractive index correction. Most of these methods are based on Snell's law[6-8]. For using Snell's law, there is need to know the beam angels before and after deflection. Some refractive index correction methods can be applied just on the homogenous and plane-parallel samples [9]. Some other methods find refractive indices in the imaging time[10]. They need some requirements such as mirror and metal plane. Moreover, there are other methods with competent results that are limited to 2D images / heterogeneous regions [11]. These methods have weak performance in the presence of speckle noise [12]. We propose a novel method for refractive index correction of OCT skin images which can be applied to the images of multi-layer, inhomogeneous and anisotropic tissues. The method does not require any initial information and pre-processing, but image of the tissue when a needle is penetrated in it. The slope of the needle through the tissue which has deflected at the boundaries, is corrected and optimum refractive indices for different layers of the skin are obtained simultaneously. This method can be widely utilized in robot assisted surgery with minimum error in locating the place of abnormality when OCT is assisting the surgery [13]. The algorithm corrects axial profiles individually which yields a corrected 2D and 3D images.

2 Materials and Methods

The OCT system used in this study is a swept-source OCT (SS-OCT) from Michelson Diagnostic™. The central wavelength of the laser is 1305 nm with a sweep range of 150 nm. The OCT is based on multi-beam technology in which four 0.25 mm width consecutive confocal gates are combined to provide a total confocal gate of 1 mm. Utilizing the multi-beam technology, the images obtained from the four channels are averaged. In the SS-OCT, the reflectivity profile is termed as an axial scan (A-scan). By grouping together several

A-lines for different transversal positions of the incident beam on the sample, a cross section image or a B-scan is generated [39]. The images obtained with this OCT system are B-Scan images with a size of 5 mm × 2 mm and software inferred C-scan images with a size of 5 mm × 5 mm. The lateral and axial resolutions of the OCT system are measured as 7.5 and 10 microns, respectively.

In the OCT system, reflected beams from sample and reference are interfered and recorded by a detector ($I_{Measured}(t)$). The image intensity at different depths is obtained based on the idea that intensity at depth Z (I_Z) is equal to $I_{Measured}$ at time t_z via the following equations:

$$Z = \frac{1}{2} C.t_Z \quad (1)$$

$$I_Z = I_{Measured}(t_Z) \quad (2)$$

where $C \propto \frac{1}{RI}$ is the speed of light in a certain medium and *RI* is the refractive index of the corresponding medium. $t_Z = t_{0:z_1} + t_{z_1:z_2} + \cdots + t_{z_{n-1}:z}$, where z_i is depth of layer *i*. For accurate image reconstruction, it is necessary to have the exact value of C or *RI* in the medium /media depending on the complexity of the tissue. This is not considered in the software of the OCT but a constant refractive index throughout the tissue. Fig.1 shows an OCT B-scan image of one layer phantom with a metal needle inside it. Since the *RI* for air and the phantom are the same in the OCT software, the straight needle seemed bent at the intersection of air and tissue.

In cases where the number of layers are more, the bending will occur at more points in the axial direction. Fig. 2 demonstrates such scenario and how the needle is straightened back after refractive index correction.

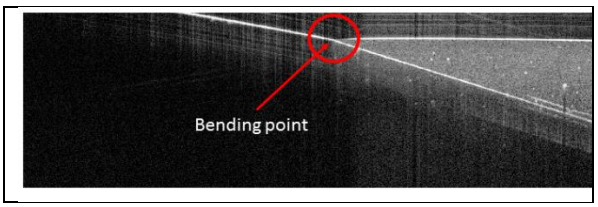

Figure 1. OCT image of one-layer pure polyurethane phantom. Bending point is where the refractive index / speed of light in media is altered.

Fig2 shows a schematic of a deflected needle at several points due to the assignment of inaccurate refractive indices. In the same figure, accurate speed of sound for each layer is used and the image compensated for refractive indices.

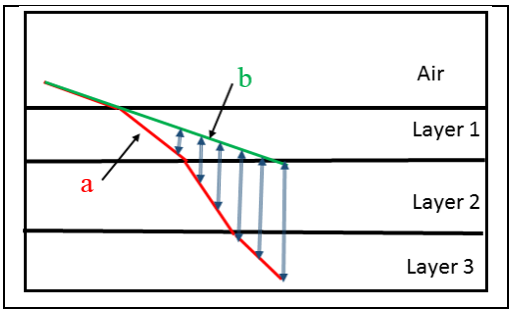

Figure 2. Schematic of refraction and the impact of inaccurate refractive index in a three-layer phantom with needle: a) Needle image before RI correction, b) Needle image after RI correction.

The proposed RI correction method in this study, employs an OCT image of the tissue into which a needle has been penetrated. There is no need for any prior information of the tissue layers or the location of boundaries. An attempt is taken to minimize the Euclidean distance between the needle image before and after *RI* correction (Eq4).

$$MSE = \frac{1}{n}\sum_n (P_{org}(n) - P_{RI-corr}(n))^2 \quad (4)$$

Where, *MSE* is mean square error, *n* is the number of pixels in the image that needs replacement, P_{org} is a vector of original pixel locations, misplaced pixel location, and $P_{RI-corr}$ is a vector of *RI* corrected pixel locations. The proposed algorithm for RI correction works for any complex tissue; heterogeneous, iso- or aniso-tropic and single or multi-layer. The algorithm works as follows. **(a)** A needle is penetrated through the tissue. The OCT image of the tissue including the needle is recorded. The RI for OCT image reconstruction is considered 1.5. **(b)** tissue layers in the OCT image are segmented [5]. **(c)** The slope of the needle in air is calculated. The needle in air is assumed to be continued into the tissue with the same slope (Figure 2). **(d)** Each A-scan is temporally modified for each depth Z_i in the image using the following equation:

$$t_i = \left(\frac{Z_1}{C_1} + \frac{Z_2}{C_2} + \cdots + \frac{Z_i}{C_i}\right) \times 2 \quad (3)$$

(e) The intensity value corresponding to the location Z_i is pulled out from the original OCT image. The initial value of refractive indices of all layers equals to 1 (refractive index of air). **(f)** The Euclidian distance between the needle image before and after RI correction is computed as MSE. MSE is minimized via changing the RI of different layers. Optimized value of RI for layers are the values which make MSE minimum.

3 Experimental results

The RI correction algorithm is applied to OCT B-scan images of one-layer and two-layer phantoms. The one-layer phantoms contain 0.1% TiO2 in polyurethane. The two-layer phantoms have one layer of 0.05% TiO2 in polyurethane and one layer of Agar gelatin on top. The results of RI correction for the one-layer phantom, and two-layer phantom, are demonstrated in Fig. 5 and Fig.6, respectively. The quantitative results are given in Table.1. RI before and after RI correction, MSE values, and the processing time are listed. The light computation of this method suggest that it can be used in real-time applications.

In our propose method, the location of pixels of each A-scan is modified separately and B-scan is finally developed with the help of all modified A-scans.

4 Conclusion

In this study, we propose a novel method for RI correction in 2D and 3D OCT images of complex tissues. The method does not require any pre-processing and can be applied to heterogeneous and anisotropic tissues. RI correction helps dermatologists to more accurately measure the thickness of skin layers and the geometry of abnormalities. The proposed method significantly reduced the misplacement of the pixels in the image.

Table1. RI correction results of two phantom OCT images.

Image	Refractive index	Processing time (s)	Type	MSE
One-layer phantom	Layer1=1.55	0.41	Org	1842
			Corr	11
Two-layer phantom	Layer1=1.55 Layer2=1.77	0.66	Org	1990
			Corr	29

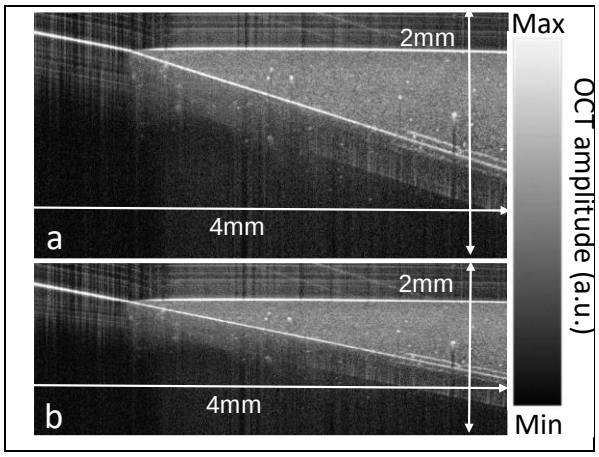

Figure 5. OCT B-scan images of one-layer polyurethane phantom into which a needle has penetrated. a) Original OCT image, b) OCT image after *RI* correction

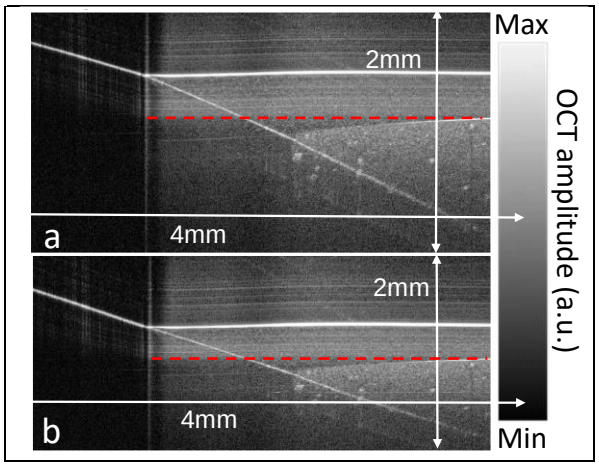

Figure 6. OCT B-scan images of two-layer polyurethane phantom into which a needle has penetrated. a) Original OCT image, b) OCT image after *RI* correction.

References

[1] J. Welzel, "Optical coherence tomography in dermatology: a review," *Skin Research and Technology*, vol. 7, pp. 1-9, 2001.

[2] M. R. Avanaki, A. Hojjatoleslami, M. Sira, J. B. Schofield, C. Jones, and A. G. Podoleanu, "Investigation of basal cell carcinoma using dynamic focus optical coherence tomography," *Applied optics*, vol. 52, pp. 2116-2124, 2013.

[3] M. R. Avanaki, A. G. Podoleanu, J. B. Schofield, C. Jones, M. Sira, Y. Liu, *et al.*, "Quantitative evaluation of scattering in optical coherence tomography skin images using the extended Huygens–Fresnel theorem," *Applied optics*, vol. 52, pp. 1574-1580, 2013.

[4] F. Hendriks, D. Brokken, C. Oomens, D. Bader, and F. Baaijens, "The relative contributions of different skin layers to the mechanical behavior of human skin in vivo using suction experiments," *Medical engineering & physics*, vol. 28, pp. 259-266, 2006.

[5] M. R. Avanaki and A. Hojjatoleslami, "Skin layer detection of optical coherence tomography images," *Optik-International Journal for Light and Electron Optics*, vol. 124, pp. 5665-5668, 2013.

[6] F. N. Golabchi, D. H. Brooks, A. Gouldstone, and C. A. DiMarzio, "Refractive effects on optical measurement of alveolar volume: A 2-D ray-tracing approach," in *Engineering in Medicine and Biology Society, EMBC, 2011 Annual International Conference of the IEEE*, 2011, pp. 7771-7774.

[7] J. Stritzel, M. Rahlves, and B. Roth, "Refractive-index measurement and inverse correction using optical coherence tomography," *Optics letters*, vol. 40, pp. 5558-5561, 2015.

[8] M. Rahlves, J. Diaz Diaz, J. Thommes, O. Majdani, B. Roth, T. Ortmaier, *et al.*, "Towards refractive index corrected optical coherence tomography as a navigation tool for bone surgery," in *Lasers and Electro-Optics Europe (CLEO EUROPE/IQEC), 2013 Conference on and International Quantum Electronics Conference*, 2013, pp. 1-1.

[9] P. H. Tomlins, P. Woolliams, C. Hart, A. Beaumont, and M. Tedaldi, "Optical coherence refractometry," *Optics letters*, vol. 33, pp. 2272-2274, 2008.

[10] G. Tearney, M. Brezinski, B. Bouma, M. Hee, J. Southern, and J. Fujimoto, "Determination of the refractive index of highly scattering human tissue by optical coherence tomography," *Optics letters*, vol. 20, pp. 2258-2260, 1995.

[11] V. Westphal, A. Rollins, S. Radhakrishnan, and J. Izatt, "Correction of geometric and refractive image distortions in optical coherence tomography applying Fermat ?? s principle," *Optics Express*, vol. 10, pp. 397-404, 2002.

[12] A. Knu and M. Boehlau-Godau, "Spatially confined and temporally resolved refractive index and scattering evaluation in human skin performed with optical coherence tomography," *Journal of Biomedical Optics*, vol. 5, pp. 83-92, 2000.

[13] X. Liu, M. Balicki, R. H. Taylor, and J. U. Kang, "Towards automatic calibration of Fourier-Domain OCT for robot-assisted vitreoretinal surgery," *Optics express*, vol. 18, pp. 24331-24343, 2010.